A LIF study on the plasma plume of a cluster of two 100 W Hall thrusters

C Royer, T Hallouin, A E Vinci, S Mazouffre

A LIF study on the plasma plume of a cluster of two 100 W Hall thrusters

IEPC-2022-378

Presented at the 37th International Electric Propulsion Conference
Massachusetts Institute of Technology, Cambridge, MA, USA
June 19-23, 2022

C. Royer
CNRS, ICARE laboratory, Orléans, France
clemence.royer@cnrs-orleans.fr

T. Hallouin
Exotrail, Massy, France
thibault.hallouin@exotrail.fr

A. E. Vinci
CNRS, ICARE laboratory, Orléans, France
alfio.vinci@cnrs-orleans.fr

S. Mazouffre
CNRS, ICARE laboratory, Orléans, France
stephane.mazouffre@cnrs-orleans.fr

This article aims to assess of the Velocity Distribution Function (VDF) in the plume of two Hall thrusters firing in cluster configuration. A cluster offers various advantages compared to a large single thruster unit: a broad operating envelope as thrusters can be fired individually or together, cost reduction as many thrusters are built, redundancy when one thruster fails, and thrust vectoring capabilities depending on the thruster arrangement. In this case, the specific impulse remains unchanged but the thrust level is the sum of the thrust of each thruster [1, 2]. A relevant point for operation is the physical interaction between the ion beam produced by each thruster. This interaction, which still is poorly grasped, certainly has an impact on the thruster performances and on the spacecraft environment. In this contribution, we experimentally examine the interaction between the plasma plumes in a cluster of two lower-power xenon-fueled Hall thrusters by means of Laser-Induced Fluorescence spectroscopy on singly-charged metastable Xe^+ ions. Those preliminary experiments clearly evidence plume overlap and ion penetration and invasion.

I. Nomenclature

α and β	=	Attenuation coefficient of lens and vacuum chamber window
$\Delta\nu$	=	Doppler shift
e	=	Elementary charge
$L_{chamber}$	=	NExET vacuum chamber
$\lambda_{exc}(vac)$	=	Laser wavelenght in vacuum
$\lambda_{fluo}(air)$	=	Fluorescence light in air
M	=	Ion mass
P_f	=	Final power density
P_{probed}	=	Probed power density
ϕ_{laser}	=	Beam diameter.
$R_{e,Larmor}$	=	Electron Larmor radius
Ud	=	Discharge voltage
ν	=	Laser frequency
ν_0	=	The frequency at rest
v	=	ion velocity
Xe^+	=	Xenon ion

II. Introduction

Since recent years, space field has witnessed SmallSat and CubeSat needs considerably growing. Throughout Starlink or OneWeb examples, the trend tends toward satellite constellation and system miniaturization. The perspective of such evolution could enhance space exploration by reducing mission cost and saving production time. Nowadays, space industry and research domains are more and more optimizing technology to benefit human knowledge and widen operation scope. Sending even more spacecraft to probe wider and further the deep space, to broader telecommunication network, improve navigation system and revive our insatiable hunger of discovery, are the main targets that lead all rocket scientists. To allow those great challenges, thrusters are mainly used for specific maneuvers like station keeping, orbit transfer, end-of-life de-orbiting,etc. Facing this challenge, new state- of-the-art devices in electric propulsion, have recently emerged as worthwhile solutions for small satellite needs.

Hall Thrusters (HTs) are ion thrusters that have already proved their reliability since decades, through various space missions. Electric propulsion and more precisely, Hall Thruster, are advantageous in terms of thrust-to-power ratio, total impulse and cost. Miniature HT are good compromises for some specific maneuvers like drag compensation or orbit correction for small platforms. HT principle relies on a magnetic lens, induced at the thruster exhaust by the help of magnet ring or coils. Electrons, emitted from an external cathode, are magnetized by the B-field. Their axial motion drops and they begin to drift azimuthally due to the ExB drift, leading to the so called Hall current. Figure 1, we can see propellant is injected upward the thruster chamber in the anode region. Neutral atoms are ionized by collision with electrons, when approaching the magnetic barrier.
Ions are pulled out of the chamber and accelerated at high velocity due to the potential difference. Magnetic strength is chosen high enough to minimize electron Larmor radius $R_{e,Larmor} \ll L_{chamber}$. It should not be too high to avoid magnetizing heavy ions.

A couple of twins ISCT100 HT has been developed to study singularity of a HT cluster system [3]. This study aims to characterize plasma plume interaction and to determine the Velocity Distribution Function (VDF) of ions, by means of laser spectroscopy. Experiment hardware and arrangement, as well as measurement procedures will be detailed in the remainder of this paper. The saturation curve of xenon-fed thruster configuration will be introduced to finally focus on a xenon-krypton approach.

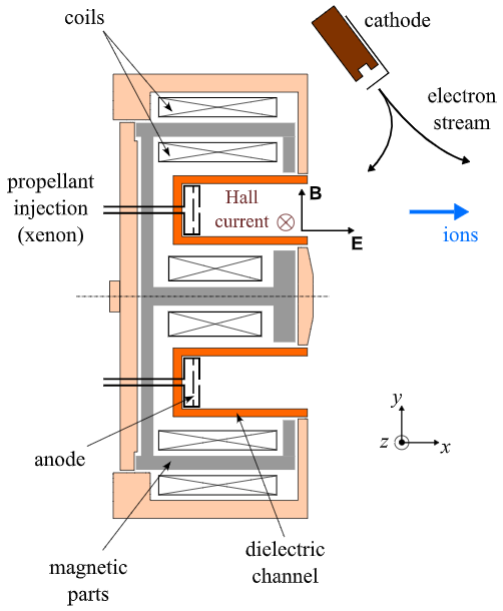

Fig. 1 Cross section view of a Hall thruster

III. Experimental diagnostic and set up

A. *LIF spectroscopy tool*

Laser-Induced Fluorescence spectroscopy (LIF) is a non-intrusive mean to probe discharge and plumes and measure ion velocity. When the entire applied potential energy is converted into kinetic energy, the ion velocity reads [4]:

$$V_{i,max} = \left(\frac{2eU_D}{M}\right)^{1/2} \tag{1}$$

Where, U_D is the discharge voltage, e, the elementary charge, M the ion mass.

A laser beam is directed toward the thruster head, along the channel axis in this work. The light source is emitting at a certain wavelength in order to excite particles and change their energy level. When particles return to their original level, they release photons, the so called fluorescence light.

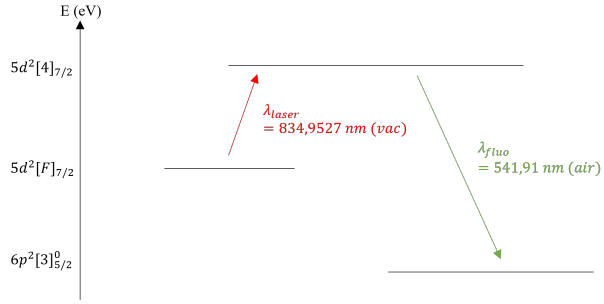

Fig. 2 Energy diagram for LIF on metastable Xe^+ ions

In the case of a metastable ion of interest here, photon of fluorescence lies in the green domain, whereas applied laser beam is set in the near infrared range, as can be seen in Figure 2. The ions velocity is given by the Doppler shift of the optical transition. The equation 2 gives the relation between laser beam wavelength.

$$\Delta\nu = \nu - \nu_0 = \frac{1}{2\pi}\mathbf{k}\cdot\mathbf{v} \tag{2}$$

Where $\Delta\nu$ is the Doppler shift, ν is the frequency, ν_0 is the frequency at rest and v the ion velocity. To determine the reference wavelength, table 1 lists ν_0 for each particles. In our study case, we will probe metastable Xe II, at the initial level $5d^2F_{7/2}$ [5].

Table 1 Current excitation and fluorescence wavelengths in LIF studies on HTs [6].

Species	Initial level	$\lambda_{exc}(vac)$	$\lambda_{fluo}(air)$
Xe II	$5d\,^2[4]_{7/2}$	834.9527	541.91
Xe I	$6s\,^2[1/2]^\circ_1$	834.9115	473.41

B. *Exprimental set up*

In this subsection, the optical bench set up will be introduced. LIF measurement uses a combination of different device to tune the red infrared laser beam. The laser beam is created by a tunable laser diode, able to deliver 700 mW power. With our laser diode the wavelength can be varied from 810 nm to 840 nm. The spectral width of the laser beam profile is about 1 MHz. While scanning over a certain laser frequency range, the beam light is continuously calibrated by a wavemeter, with an accuracy of 80 MHz (≈60m/s). Moreover, a scanning confocal Fabry-Perot interferometer of 1GHz free spectral range is highly required to monitor undesirable "mode hops" event which could affect the quality of

the laser. The primary laser beam is modulated by a mechanical chopper at a frequency ~1 kHz before being coupled into a half-wave plate and a polarizer to change the beam polarization if needed. Here, the beam was vertically polarized for all measurements. A schematic of the optical bench is shown in figure 3. [7].

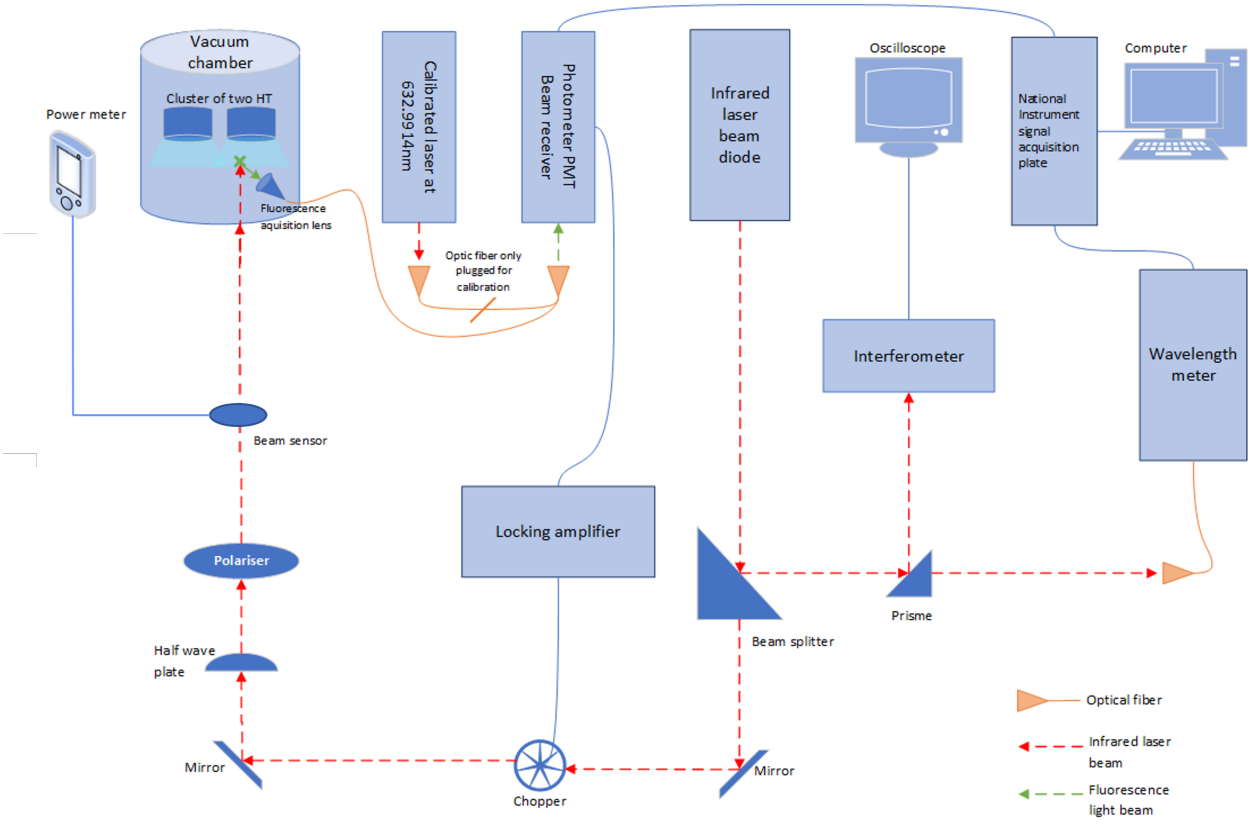

Fig. 3 LIF set up schematic

The infrared laser is headed axially toward the plasma and aligned with the channel axis of one of the two thrusters of the cluster. This specific configuration allow to determine the axial velocity component of the ions in the plume.

As shown in figure 4, a focal lens is mounted directly inside the vacuum chamber and set below the cluster of two HT. Focal length is 40 mm. It is absorbing and delivering the fluorescence light through a 200 μm optical fiber. The acquired fluorescence beam lies in the visible domain at a wavelength of λ_{fluo} = 541.91 nm. This value is set on a monochromator and remains unchanged during the whole experiment. The fluorescence light is filtered through a 20 cm focal length monochromator, to isolate fluorescence frequency from the rest of the spectrum. The focal point is crossing the laser beam and the plasma plume. Acquisition point is shifted closer or further away from the HT exhaust area by the need of two axial translation as can be seen in Figure 4. For time-averaged LIF measurements, a lock-in amplifier operating at the chopper frequency is used to discriminate the fluorescence light from the intrinsic plasma emission. Scanning of the laser diode cavity, data acquisition and laser wavelength monitoring are of course computer controlled.

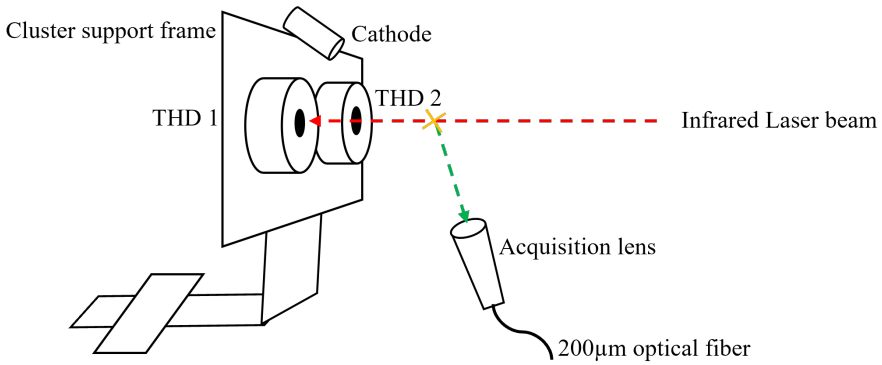

Fig. 4 Schematic of the LIF method inside the vacuum tank.

The fluidic system is detailed in Figure 5. A set of two mass flow controllers allow us to switch between a full xenon fed system to a hybrid system with xenon and krypton. In the latter case, Thruster Head (THD) 1 is fed with krypton while THD 2 operates with xenon as propellant. The remaining mass flow controller is dedicated to bring xenon to the cathode for the two thrusters.

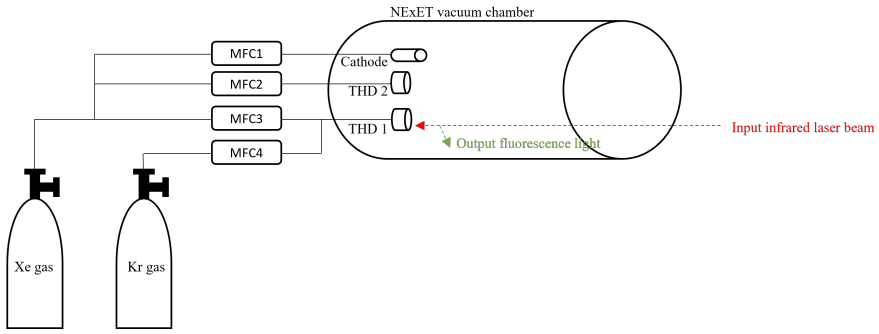

Fig. 5 Vacuum chamber fluidic system schematic.

C. *Cluster configuration*

For our study purpose, a set of two identical 100 W-class ISCT100 Hall Thrusters have been installed on a frame inside the NExET vacuum chamber, at the CNRS-ICARE laboratory. Background pressure remains at 10^{-7} mbar whenever thrusters aren't firing, whereas pressure increases to 10^{-4} mbar when two thrusters are simultaneously operated. A schematic of the set up and thruster assembly is depicted in Figure 5.

Two power-supplies have been used to power each thruster. Primary power-supply is a Delta Elektronika device. It polarizes positively the anode of the Thruster Head 1 (THD 1) and the common cathode keeper. Keeper potential is manually switched at low frequency. The THD 2 anode is supplied by a Keithley power-supply. The discharge circuit is closed through the heater minus. Whenever, ignition is induced, keeper switching potential is turned off.
The common cathode is a 5 A-class hollow cathode with a LaB6 emitter [8] and is operating for either a cluster configuration or a single-thruster configuration. The heater is continually powered by a high current EA-PSI power-supply at 18A and 21V. The power range varies from 360 W to 400 W. Conditions are given in Table 2.
In previous study, operating a single cathode in a cluster has been compared with a multiple cathode layout. When operating multiple cathodes, it seems that one is dominating to furnish electron current. There is not real differences in plasma potential between a shared cathode and multiple cathode configurations[9]. Moreover, no relevant change in performance is observed when cathode-cluster position is increased. [10].

During the entire campaign, each thruster has been operating at the same working point. Parameters are listed in Table 2:

Table 2 Hollow cathode parameters.

Heater voltage limit [V]	Heater nominal applied current [A]	Maximum heater power [W]	Cathode mass flow [sccm]	Heating process
22	18	400	2.5	The heater is gradually heated at 2.5 A/min speed

Table 3 Single Hall thruster parameters [11].

Stage	Applied discharge voltage [V]	Discharge current threshold [A]	Maximum HT power [W]	Anode mass flow [sccm]
Ignition	500	0.3	150	9
Operation	200	0.85	170	12

Regarding the study parameters, we can evaluate the maximum Xe^+ velocity, when no energy loss is taking into account. Equation (1) leads to $V_{i,max,\infty} \approx 17.1$ km/s.

To lead this study, six cases have been examined. For all cases, LIF measurements have been performed at x = 20 mm along the channel axis of THD 1 (knowing that x = 0 mm refers to the exit plane).

1) Single mode : THD 1 is firing with xenon, no gas is injected or ionized in the THD 2 channel.
2) Cluster mode : Both THD are operating with similar parameters and supplied with xenon gas.
3) Cluster mode : THD 1, supplied with krypton and THD 2 with xenon.
4) Single mode : THD 1 is supplied with krypton gas without plasma discharge, whereas THD 2 is firing with xenon.
5) Single mode : THD 1 is operating with krypton, THD 2 is supplied with xenon gas without plasma discharge.
6) Single mode : THD 1 is operating with krypton, no operation or gas injection for THD 2.

Cases and configuration are illustrated in Figure 6.

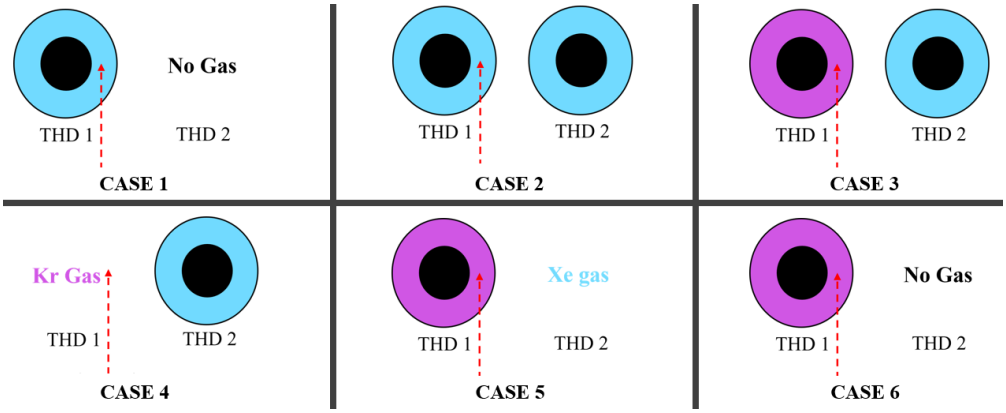

Fig. 6 Various cluster configurations. LIF on Xe^+ ions is solely performed along the axis of THD 1 at x = 20 mm.

D. *Saturation of the optical transition*

LIF is a reliable tool when one needs to assess Ion Velocity Distribution Function. Laser spectroscopy avoid in situ measurement which can contaminate the plasma plume or induce a change in plasma potential. In order to determine accurately the ion VDF[12], the Doppler-shifted spectral line must not be perturbed by saturation broadening. This phenomenon is an instrumental effect when laser power intensity is over scaled. In his review, M. J. Goeckner explains that saturation occurs when the stimulated photon emission rate is equivalent to the photon absorption rate and greater than the spontaneous photon emission rate. When saturation occurs, the measured fluorescence line is broadened [13] . This is known as saturation or power broadening.

Saturation of the metastable Xe^+ optical transition used in this study has been experimentally invetigated. Through all the optic path, laser power is drastically reduced from the laser diode output to the inner vacuum chamber. Following the figure 3, a power meter is place at the end of the optic path, in front of the chamber window in the air side. An attenuation percentage of 10% is taken into account to calculate the final laser power, in the measurement volume.

$$P_f = 2\alpha\beta\frac{P_{probed}}{\pi\phi_{laser}^2/4} \tag{3}$$

Where P_f is the final power density which excites Xe^+, α and β are the attenuation coefficient of lens and vacuum chamber window, P_{probed} is the probed power measured by the powermeter and ϕ_{laser} is the beam diameter. The factor 2 account for the chopper attenuation.

The laser power in the measurement volume has been varied from 5mW to 40mW. The LIF signal is then computed from integration of the measured line profile. Figure 7 shows the LIF signal as a function of the laser power. The signal increases linearly from 0 up to about 12 mW. Above this value the evolution is no more linear and the saturation domain is reached. Referring to the evolution of the LIF signal, saturation seems to occurs at $12mW$, under our conditions at x = 0 mm. Hence, to avoid disturbing the fluorescence lineshape, 12 mW has been continuously taken to perform measurements in the remainder of this work.

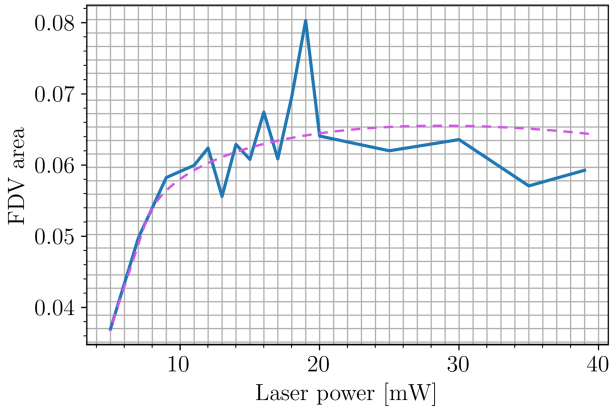

Fig. 7 Metastable Xe^+ optical transition saturation.

IV. Xe ion axial VDF

A. *Single HT case*

In this section, we will review first set of measurements, performed on a single THD, supplied with xenon gas. The first case configuration is exemplified in Figure 8. Figure 9 - 14 show the normalized LIF spectral profile that images the Xe^+ ion VDF to a large extend as previously explained [14]. The unit of the horizontal axis is the velocity unit here instead of the wavelength unit to directly access the ion most probable velocity. The axis unit has been converted using the Doppler shift formula. The laser range used to probe Xe^+ ion velocity profile extends from 834.9527 nm to 835.0223 nm, according to Equation 2. The Doppler shift corresponds to a particle velocity range of 0 km/s to 25 km/s

The measured LIF spectra exhibit the standard Gaussian-like shape for a Hall thruster plume. Small peaks in the wings could be due to a weak quality of the laser beam profile. Indeed during this work the laser appeared to be quite unstable with frequent mode hops.
Figure 15 shows the on-axis development of the most probable Xe^+ ion velocity. The ion velocity increases when moving downstream. The largest ion velocity stays below the maximum achievable velocity at 200 V applied voltage, i.e. 17,1 km/s, indicating losses. As expected a large fraction of the acceleration process occurs outside the HT cavity. The width of the velocity profile also decreases when the distance to the exit plane increases. This is due to overlap between the ionization and acceleration layers. [13].

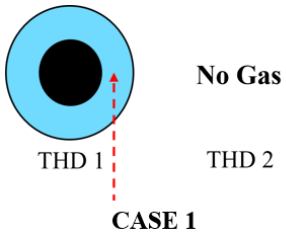

Fig. 8 figure
Case 1 disposition.

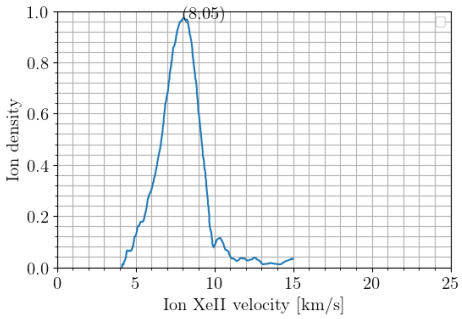

Fig. 9 figure
Case 1 VDF at 0mm.

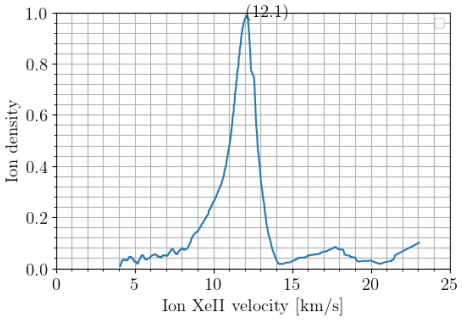

Fig. 10 figure
Case 1 VDF at 4mm.

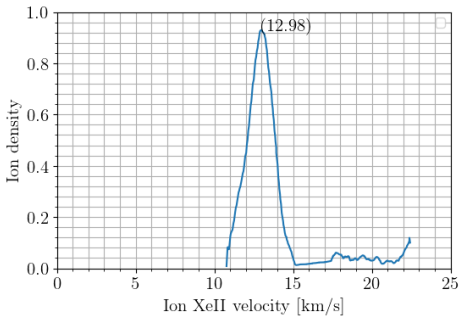

Fig. 11 figure
Case 1 VDF at 10mm.

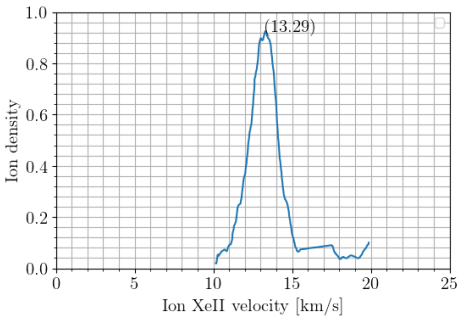

Fig. 12 figure
Case 1 VDF at 14mm.

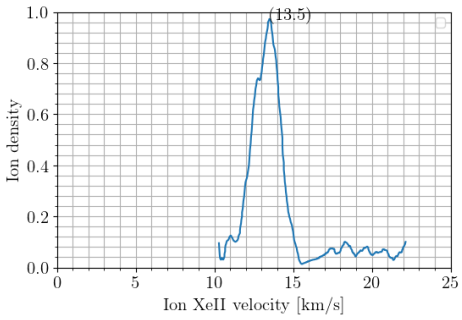

Fig. 13 figure
Case 1 VDF at 18mm.

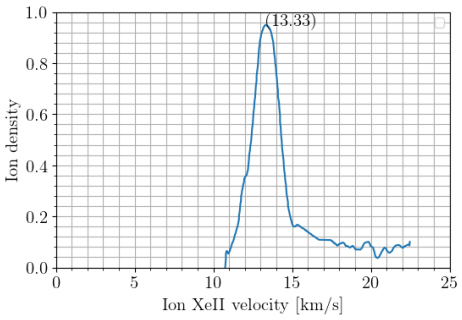

Fig. 14 figure
Case 1 VDF at 22mm.

B. *Cluster and plume interaction*

A LIF investigation has been performed on a cluster of two ISCT100 Hall thrusters with a common cathode. The configuration of the experiment is shown in Figure 16. To the best of our knowledge, LIF spectroscopy has never been applied to a cluster of two low-power Hall thrusters.

LIF measurements have been carried out at different positions in cluster configuration. Shifts in velocity, compared to single HT configuration, are observed but not relevant to assume any performance influence of the cluster mode on the Xe^{+} velocity. LIF measurements have been carried out at different positions in cluster configuration.
Change in background pressure between the single-HT and cluster modes could explained the change in velocity. The pressure level is almost double in cluster configuration ion in this work, which certainly has an effect on both the ionization and acceleration process. This work is preliminary as previously mentioned. In order to make more precise and definitive conclusions, the background pressure should be kept the same in single-HT and cluster configuration not to affect physical processes.

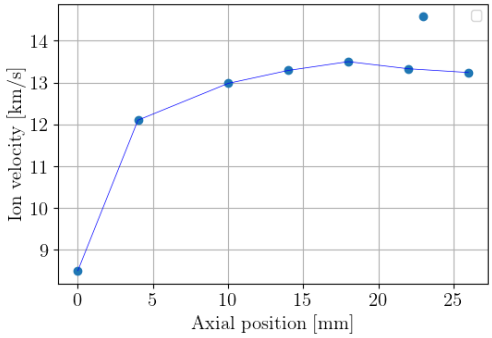

Fig. 15 figure
Most probable ion velocity against axial position for case 1.

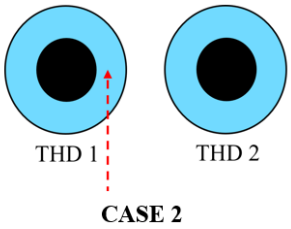

Fig. 16 figure
Case 2 disposition.

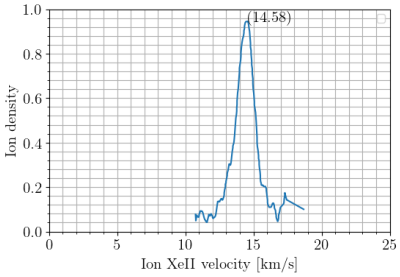

Fig. 17 figure
Case 1 : single thruster VDF at 23mm.

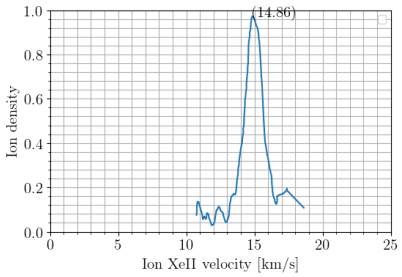

Fig. 18 figure
Case 2 : cluster of thwo thrusters VDF at 23mm.

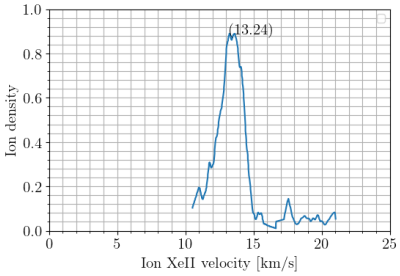

Fig. 19 figure
Case 1 : single thruster VDF at 26mm.

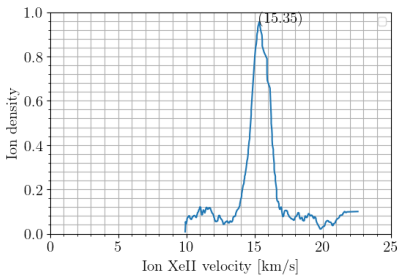

Fig. 20 figure
Case 2 : cluster of thwo thrusters VDF at 26mm.

V. Cluster plume invasion

We finally investigated cases 3-4 in cluster configuration. Figure 21 is a reminder of the case configurations. Two inert gas has been used to supply thrusters of the cluster : krypton and xenon. The laser is shined along the channel axis of THD 1 and measurements were performed at x = 20 mm. Although krypton plasma discharge and plume are generated, LIF spectroscopy was only used to detect Xe^+ ions. For our purpose, krypton is used to recreate boundary condition of an ionized gas medium when laser spectroscopy is used to probe Xe^+ ions in THD 1.

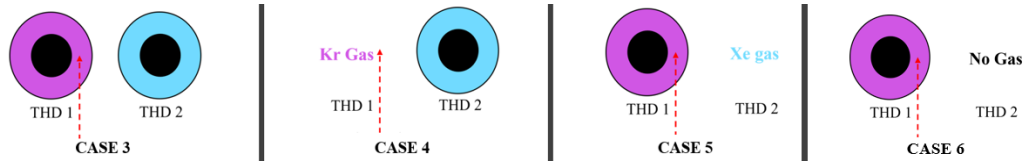

Fig. 21 figure
Case 3, 4, 5.

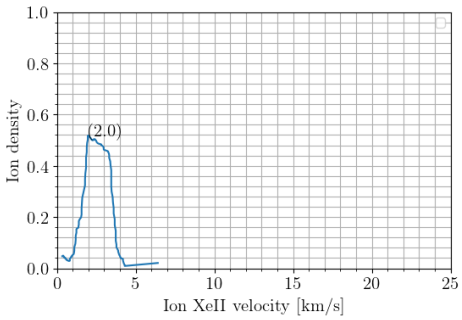

Fig. 22 figure
Case 3 : VDF at 20mm.

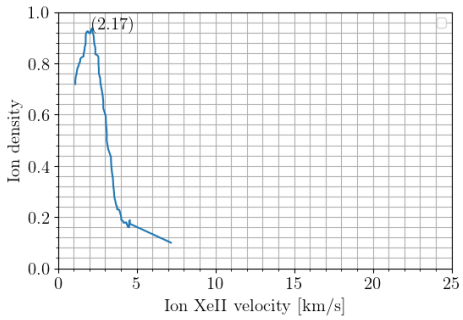

Fig. 23 figure
Case 5 : VDF at 20mm.

Figure 22 corresponds to the Xe^+ ion velocity profile measured in case 3 when THD 1 operates with krypton and THD 2 with xenon. Two discharges are created here. Peak is measured inside the krypton plasma plume of the THD 1. Based on this unique outcome, one might conclude that observed Xe^+ ions may originate from the xenon plasma of the THD 2.

Figure 23 corresponds to the Xe^+ ion velocity profile measured in case 5 when THD 1 operates with krypton and THD 2 is fed with xenon without a plasma discharge. As can be seen, a slow ion peak is also observed by LIF in these conditions. The signal is even higher in case 5 compared to case 3. In this specific case, only xenon gas is released from THD 2, which is not ignited. This result is a bit surprising as it was supposed to be found in the case 5, knowing that THD 2 wasn't firing in this configuration. These two measurements show that Xe ions and Xe atoms from one thruster can penetrate and invade the plume of a second thruster placed in the surroundings. This might be the first evidence of a plume invasion phenomenon in a HT cluster.

No Xe^+ ion signal was recorded in case 6 when the cluster heads are not fed with xenon. This case is nevertheless interesting and relevant as it also indicates that no ions (at least in a metastable state) from the cathode are detected in the HT plume. Finally, case 4 with THD 1 supplied with krypton but without creating a plasma discharge and THD 2 firing with xenon must be discussed. One could expect a Xe^+ ion LIF signal on THD 1 channel axis as this case is quite similar to case 3. However, no signal was observed. There is only one possible explanation. Ions observed in case 3 originate from the local ionization (in THD 1 plume or ionization region) of xenon atoms leaving THD 2. The fact that the LIF signal is larger in case 5 than in case 3 supports this point as the atom density is larger without plasma discharge for a given gas flow rate. Moreover, outcomes of case 4 also show that the atom flow from the cathode does not impact much the plume of a Hall thruster.

VI. Conclusion

This work is the first investigation of Hall thruster plume interaction in a cluster configuration by means of LIF spectroscopy on ions. Experiments have been carried out on metastable Xe^+ ions in the plasma plume of two low-power miniature ISCT100 Hall thrusters in cluster configuration with a single cathode. Xenon and krypton have been used as propellant gas. Preliminary results show the invasion and penetration phenomena as particles from one thruster are detected in the plume of neighboring thruster. This study shows in addition that the cathode gas flow does not interact much with the thruster plume.

Acknowledgments

C. Royer benefits from a CNES/Exotrail Ph.D. grant. This study was performed within the framework of the ORACLE joint-laboratory program.

References

[1] Walker, M. L., and Gallimore, A. D., "Performance characteristics of a cluster of 5-kW laboratory Hall thrusters," *Journal of Propulsion and Power*, Vol. 23, No. 1, 2007, pp. 35–43.

[2] Lobbia, R. B., and Gallimore, A. D., "Performance measurements from a cluster of four Hall thrusters," *30th International Electric Propulsion Conference, Florence, Italy*, 2007.

[3] Mazouffre, S., and Grimaud, L., "Characteristics and performances of a 100-W Hall thruster for microspacecraft," *IEEE Transactions on Plasma Science*, Vol. 46, No. 2, 2018, pp. 330–337.

[4] Boeuf, J.-P., "Tutorial: Physics and modeling of Hall thrusters," *Journal of Applied Physics*, Vol. 121, No. 1, 2017, p. 011101.

[5] Lejeune, A., Bourgeois, G., and Mazouffre, S., "Kr II and Xe II axial velocity distribution functions in a cross-field ion source," *Physics of Plasmas*, Vol. 19, No. 7, 2012, p. 073501.

[6] Vinci, A. E., and Mazouffre, S., "Laser-induced fluorescence spectroscopy on xenon atoms and ions in the magnetic nozzle of a helicon plasma thruster," *submitted to Plasma Source Science and Technology, 2022*, 2022.

[7] Mazouffre, S., "Laser-induced fluorescence diagnostics of the cross-field discharge of Hall thrusters," *Plasma Sources Science and Technology*, Vol. 22, No. 1, 2012, p. 013001.

[8] Potrivitu, G.-C., Joussot, R., and Mazouffre, S., "Anode position influence on discharge modes of a LaB6 cathode in diode configuration," *Vacuum*, Vol. 151, 2018, pp. 122–132.

[9] Beal, B. E., Gallimore, A. D., and Hargus Jr, W. A., "Effects of cathode configuration on hall thruster cluster plume properties," *Journal of Propulsion and Power*, Vol. 23, No. 4, 2007, pp. 836–844.

[10] Walker, M. L., and Gallimore, A. D., "Hall thruster cluster operation with a shared cathode," *Journal of Propulsion and Power*, Vol. 23, No. 3, 2007, pp. 528–536.

[11] Hallouin, T., and Mazouffre, S., "Far-field plume characterization of a 100-W class Hall thruster," *Aerospace*, Vol. 7, No. 5, 2020, p. 58.

[12] Goeckner, M., and Goree, J., "Laser-induced fluorescence measurement of plasma ion temperatures: Corrections for power saturation," *Journal of Vacuum Science & Technology A: Vacuum, Surfaces, and Films*, Vol. 7, No. 3, 1989, pp. 977–981.

[13] Mazouffre, S., "Laser-induced fluorescence spectroscopy applied to electric thrusters," *Von Karman Institute for Fluid Dynamics, STO-AVT-VKI Lecture series 263*, 2016, pp. p–10.

[14] Cusson, S. E., Georgin, M. P., Dragnea, H. C., Dale, E. T., Dhaliwal, V., Boyd, I. D., and Gallimore, A. D., "On channel interactions in nested Hall thrusters," *Journal of Applied Physics*, Vol. 123, No. 13, 2018, p. 133303.